Protein Science (1997), *6*:2084–2096. Cambridge University Press. Printed in the USA.

Unusual conformation of nicotinamide adenine dinucleotide (NAD) bound to diphtheria toxin: A comparison with NAD bound to the oxidoreductase enzymes

CHARLES E. BELL,[1] TODD O. YEATES, AND DAVID EISENBERG

UCLA-DOE Laboratory of Structural Biology and Molecular Medicine, Molecular Biology Institute, and Department of Chemistry and Biochemistry, University of California at Los Angeles, Los Angeles, California 90095-1569

(RECEIVED January 13, 1997; ACCEPTED June 12, 1997)

Abstract

The conformation of NAD bound to diphtheria toxin (DT), an ADP-ribosylating enzyme, has been compared to the conformations of NAD(P) bound to 23 distinct NAD(P)-binding oxidoreductase enzymes, whose structures are available in the Brookhaven Protein Data Bank. For the oxidoreductase enzymes, NAD(P) functions as a cofactor in electron transfer, whereas for DT, NAD is a labile substrate in which the N-glycosidic bond between the nicotinamide ring and the N-ribose is cleaved. All NAD(P) conformations were compared by (1) visual inspection of superimposed molecules, (2) RMSD of atomic positions, (3) principal component analysis, and (4) analysis of torsion angles and other conformational parameters. Whereas the majority of oxidoreductase-bound NAD(P) conformations are found to be similar, the conformation of NAD bound to DT is found to be unusual. Distinctive features of the conformation of NAD bound to DT that may be relevant to DT's function as an ADP-ribosylating enzyme include (1) an unusually short distance between the PN and N1N atoms, reflecting a highly folded conformation for the nicotinamide mononucleotide (NMN) portion of NAD, and (2) a torsion angle $\chi_N \sim 0°$ about the scissile N-glycosidic bond, placing the nicotinamide ring outside of the preferred anti and syn orientations. In NAD bound to DT, the highly folded NMN conformation and torsion angle $\chi_N \sim 0°$ could contribute to catalysis, possibly by orienting the C1′N atom of NAD for nucleophilic attack, or by placing strain on the N-glycosidic bond, which is cleaved by DT. The unusual overall conformation of NAD bound to DT is likely to reflect the structure of DT, which is unusual among NAD(P)-binding enzymes. In DT, the NAD binding site is formed at the junction of two antiparallel β-sheets. In contrast, although the 24 oxidoreductase enzymes belong to at least six different structural classes, almost all of them bind NAD(P) at the C-terminal end of a parallel β-sheet. The structural alignments and principal component analysis show that enzymes of the same structural class bind to particularly similar conformations of NAD(P), with few exceptions. The conformation of NAD bound to DT superimposes closely with that of an NAD analogue bound to *Pseudomonas* exotoxin A, an ADP-ribosylating toxin that is structurally homologous to DT. This suggests that all of the ADP-ribosylating enzymes that are structurally homologous to DT and ETA will bind a highly similar conformation of NAD.

Keywords: diphtheria toxin; NAD conformation; nicotinamide adenine dinucleotide (NAD); principal component analysis; Rossmann fold; Structural Classification of Proteins (SCOP) database

Reprint requests to: David Eisenberg, UCLA-DOE Laboratory of Structural Biology and Molecular Medicine, Molecular Biology Institute, and Department of Chemistry and Biochemistry, Box 951569, University of California at Los Angeles, Los Angeles, California 90095-1569; e-mail: david@pauling.mbi.ucla.edu.

[1]Present address: University of Pennsylvania, Department of Biochemistry & Biophysics, School of Medicine, Philadelphia, Pennsylvania 19104-6059.

Abbreviations: NAD, nicotinamide adenine dinucleotide; NADP, nicotinamide adenine dinucleotide 3′-phosphate; NAD(P), NAD or NADP; DT, diphtheria toxin; EF-2, elongation factor 2; RMSD, root-mean-squared deviation; NMN, nicotinamide mononucleotide portion of NAD; AMP, adenosine monophosphate portion of NAD; SCOP, Structural Classification of Proteins database; PDB, Brookhaven Protein Data Bank; ETA, *Pseudomonas* exotoxin A; β-TAD, β-methylene-thiazole-4-carboxamide adenine dinucleotide.

Nature commonly uses nicotinamide adenine dinucleotide and nicotinamide adenine dinucleotide 3′-phosphate as cofactors for enzymes that catalyze biological reactions involving electron transfer. In these reactions, a hydride ion is transferred to or from the C4 atom of the nicotinamide ring of NAD(P), resulting in either the reduction or oxidation of a substrate molecule. Over the past 30 years, the atomic structures of the NAD(P)-bound forms of at least 23 distinct oxidoreductase enzymes have been determined to atomic resolution by X-ray crystallography. Although at least 14 of the NAD(P)-binding oxidoreductase enzymes whose structures have been determined in complex with NAD(P) have the well-known dinucleotide-binding fold, also called the Rossmann fold (Rossmann et al., 1975), at least five other types of folds have emerged for enzymes of this function. For example, aldose reductase has an $(\alpha\beta)_8$ structure (Wilson et al., 1992) that is quite different from the Rossmann fold. The 23 distinct oxidoreductase enzymes for which an NAD(P)-bound structure has been determined and deposited in the Brookhaven Protein Data Bank are listed in Table 1. In this table, the 23 NAD(P)-binding oxidoreductase enzymes have been segregated into six classes on the basis of their folding topologies. The classification into distinct structures in Table 1 is taken directly from the Structural Classification of Proteins database, release 1.32 (Murzin et al., 1995), although the class numbers have been assigned by the present authors. A representative structure for each of the six structural classes of NAD(P)-binding oxidoreductase enzymes is shown in Figure 1.

Recently, we have determined the crystal structure of the NAD complex of diphtheria toxin [DT (Bell & Eisenberg, 1996)], an NAD-binding protein that utilizes NAD as a labile substrate rather than as a cofactor for electron transfer (Fig. 2). Specifically, DT catalyzes the covalent transfer of the ADP-ribose portion of NAD to a diphthamide residue (posttranslationally modified histidine; Van Ness et al., 1980) of elongation factor-2, causing inhibition of protein synthesis and cell death (Collier, 1975). This reaction involves the cleavage of NAD at the N-glycosidic bond between the nicotinamide ring and the N-ribose. In the absence of EF-2, DT also catalyzes the hydrolysis of NAD at the N-glycosidic bond, although at a rate of only one per minute (Lory et al., 1980). The crystal structures of at least five other ADP-ribosylating enzymes have been determined, although their NAD complexes have not. The crystal structure of *Pseudomonas* exotoxin A, which catalyzes the same ADP-ribosylation reaction as DT, has been determined in complex with an NAD analogue (Li et al., 1996).

Because the function of DT, an ADP-ribosylating enzyme, is unique among the group of 24 enzymes whose structures have been determined in complex with NAD(P), one might expect to find differences in the conformation of NAD when bound to DT that may be relevant to DT's unique function. In order to gain insight into DT's function as an ADP-ribosylating enzyme, we have compared the conformation of NAD bound to DT, to the conformations of NAD(P) bound to the 23 oxidoreductase enzymes available in the PDB. We have compared all NAD(P) conformations by (1) visual examination of superimposed structures, (2) RMSD in atomic positions, (3) principal component analysis, and (4) comparison of torsion angles and other conformational parameters.

In previous studies, the similarity in conformation of bound NAD(P) among the dehydrogenase enzymes having the Rossmann fold has been well documented (Rossmann et al., 1975; Branden & Eklund, 1980; Grau, 1982; Eklund & Branden, 1987). In addition,

Table 1. *Crystal structures of enzymes bound to NAD(P) available in the Brookhaven Protein Data Bank*[a]

Class	Enzyme	PDB	Res (Å)	Ligand	Source
1	Alcohol dehydrogenase	2OHX	1.8	NAD	Horse liver
1	Quinone oxidoreductase	1QOR	2.2	NADP	*E. coli*
1	3-α 20-β-Hydroxysteroid dehydrogenase	2HSD	2.6	NAD	*Streptomyces hydrogenans*
1	Dihydropteridine reductase	1DHR	2.3	NAD	Rat liver
1	Enoyl-ADP-reductase	1ENY	2.2	NAD	Mycobacterium tuberculosis
1	Glyceraldehyde-3-P dehydrogenase	1GAD	1.8	NAD	*E. coli*
1	Dihydrodipicolinate reductase	1DIH	2.2	NADP	*E. coli*
1	Formate dehydrogenase	2NAD	2.0	NAD	*Pseudomonas sp.*
1	Phosphoglycerate dehydrogenase	1PSD	2.8	NAD	*E. coli*
1	D-Lactate dehydrogenase	2DLD	2.7	NAD	*Lactobacillus helveticus*
1	Malate dehydrogenase	1BMD	1.9	NAD	*Thermus flavus*
1	L-2-Hydroxyisocaproate dehydrogenase	1HYH	2.2	NAD	*Lactobacillus confusus*
1	Lactate dehydrogenase	9LDT	2.0	NAD	Porcine muscle
1	6-phosphogluconate dehydrogenase	1PGO	2.5	NADP	Sheep
2	Glutathione reductase	1GRB	2.0	NADP	Human erythrocytes
2	Thioredoxin reductase	1TDF	2.3	NADP	*E. coli*
2	NADH peroxidase	2NPX	2.4	NAD	*Streptococcus faecalis*
2	Dihydrolipoamide dehydrogenase	1LVL	2.5	NAD	*Pseudomonas putida*
3	Aldose reductase	1ADS	1.6	NADP	Human placenta
4	3-Isopropylmalate dehydrogenase	1HEX	2.5	NAD	*Thermus thermophilus*
4	Isocitrate dehydrogenase	1IKB	2.5	NADP	*E. coli*
5	Catalase	8CAT	2.5	NADP	Beef liver
6	Dihydrofolate reductase	8DFR	1.7	NADP	Chicken liver
7	Diphtheria toxin	1TOX	2.3	NAD	*Corynebacterium diphtheriae*

[a]Classes in column 1 are from the SCOP database (Murzin et al., 1995), with identifying numbers added by the present authors. Column 3 gives the PDB identification codes.

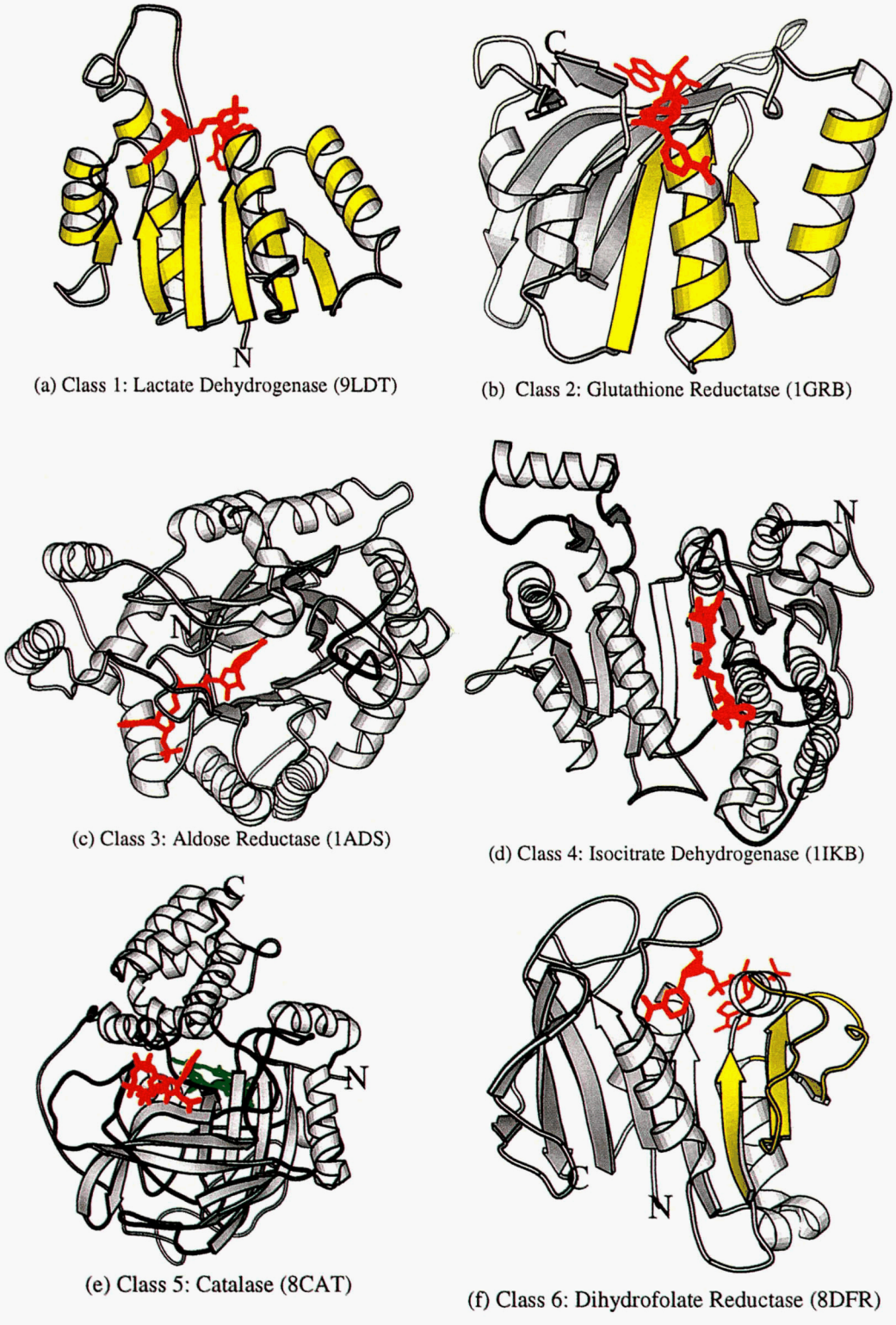

(a) Class 1: Lactate Dehydrogenase (9LDT)

(b) Class 2: Glutathione Reductatse (1GRB)

(c) Class 3: Aldose Reductase (1ADS)

(d) Class 4: Isocitrate Dehydrogenase (1IKB)

(e) Class 5: Catalase (8CAT)

(f) Class 6: Dihydrofolate Reductase (8DFR)

Fig. 1. The six structural classes of NAD(P)-binding oxidoreductase enzymes, listed in the SCOP database (Murzin et al., 1995), with numbering by the present authors. For each of the six structural classes (see Table 1), one representative structure is shown (**A**–**F**). For each structure, NAD(P) is shown in red lines. In (**A**), the Rossmann fold is shown in yellow. In (**B**) and (**F**), the mononucleotide binding fold (1/2 of the Rossmann fold) is also shown in yellow. In (**E**), the heme group bound to catalase is shown in green lines. In (**A**) and (**B**), only the NAD binding domains are shown. Notice that, except for NADP bound to catalase (**E**), in all protein structures the NAD(P)-binding site is located at the C-terminal end of a parallel β-sheet. The figure was prepared using MOLSCRIPT (Kraulis, 1991).

Fig. 2. Structure of the catalytic domain of diphtheria toxin bound to NAD. The catalytic domain of DT [PDB entry 1TOX (Bell & Eisenberg, 1996)] is shown in ribbon representation and NAD is shown in black lines. Notice that the NAD-binding site is located at the surface of two antiparallel β-sheets, which meet at approximately a right angle.

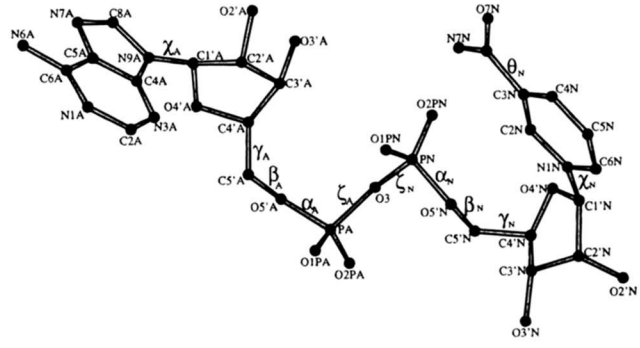

Fig. 3. Conformation of NAD bound to diphtheria toxin. All atom names are labeled, and torsion angles defined, according to current IUPAC-IUB nomenclature (IUPAC-IUB Joint commission on biochemical nomenclature. 1983. *Eur J Biochem 131*:9–15), except for the ζ angles. The χ_N torsion angle is defined by the positions of C2N-N1N-C1′-N-O4′N. The γ_A and γ_N torsion angles are defined by the positions of C3′-C4′-C5′-O5′. The χ_A torsion angle is defined by the positions of C4A-N9A-C1′A-O4′A.

the conformations of unbound nucleotides, including NAD(P), FAD, FMN, FAD, ATP, and others, were compared to their conformations when bound to enzymes, in terms of torsion angles (Moodie & Thornton, 1993). It was observed that the enzyme-bound nucleotides tend to adopt an extended or "open" conformation, whereas unbound nucleotides prefer a more "closed" conformation. An explanation offered for this observation (Moodie & Thornton, 1993) was that the extended conformation of bound nucleotides allows for more interactions with residues of the enzyme.

In this study, we focus on comparing the conformation of NAD bound to DT, an ADP-ribosylating enzyme, to the conformations of NAD(P) bound to 23 oxidoreductase enzymes.

Results

Conformation of NAD bound DT

The conformation of NAD bound to DT is shown in Figure 3, with atoms and relevant torsion angles labeled. In the crystal structure of DT (Bell & Eisenberg, 1996), there are two DT-NAD complexes in the asymmetric unit of the crystal, and thus there are two independent determinations of the conformation of NAD bound to DT. However, because the two independently determined conformations of NAD bound to DT align to an RMSD of only 0.33 Å and are thus nearly identical, only one of the NAD conformations (molecule one of the asymmetric unit) will be used for most of the comparisons in this study.

Overall, the conformation of NAD bound to DT can be described as extended (Fig. 3): the AC6 to NC2 distance between the adenine and nicotinamide rings, which is used frequently as a measure of the overall extension of a particular NAD(P) conformation (Webb et al., 1973; Rossmann et al., 1975; Ecklund et al., 1984), is 12.5 Å. The nicotinamide mononucleotide portion, however, is in a highly folded, or "closed" conformation. The nicotinamide ring is in approximately the syn orientation ($\chi_N \sim 0°$), placing the carboxamide group of the nicotinamide ring over the N-ribose. In addition, the γ_N torsion angle (O5′-C5′-C4′-C3′) is at $-75°$, placing the N-phosphate over the N-ribose. The N-ribose is in the C3′-endo conformation. The "closed" conformation of the NMN portion of NAD bound to DT allows for the formation of a hydrogen bond between the N-phosphate and the carboxamide group of nicotinamide.

In contrast, the adenosine monophosphate portion of NAD bound to DT is more extended. The $\gamma_A \sim -114°$ torsion angle places the A-phosphate away from the A-ribose. The A-ribose is in the C2′-endo conformation. The adenine ring is in the syn orientation ($\chi_A \sim 73°$), placing the six-membered ring of adenine over the A-ribose.

Superposition of enzyme-bound NAD(P) conformations

As a first step toward comparing the conformation of NAD bound to DT to the other enzyme-bound NAD(P) conformations in Table 1, all enzyme-bound NAD(P) conformations have been superimposed by least squares (Fig. 4A) and the RMSD values between each pair of enzyme-bound NAD(P) structures have been calculated (Table 2). As seen in the superposition in Figure 4A, the conformation of NAD bound to DT is unusual: the conformations of NAD(P) bound to 22 of the oxidoreductase enzymes all follow a similar path, whereas the DT-bound NAD conformation deviates from this path significantly. As viewed in the superposition in Figure 4A, the oxidoreductase-bound NAD(P) conformations are particularly similar at the AMP portion, whereas the DT-bound NAD conformation is clearly different. At the NMN portion, the 22 conformations of NAD(P) bound to oxidoreductase enzymes show less similarity.

The unusual conformation of NAD bound to DT is also evident from the RMSD values in Table 2 (1TOX in last column). In Table 2, RMSD values are presented between each of the 24 enzyme-bound NAD conformations (rows 1–24) and a representative NAD(P) conformation for each of the six structural classes of

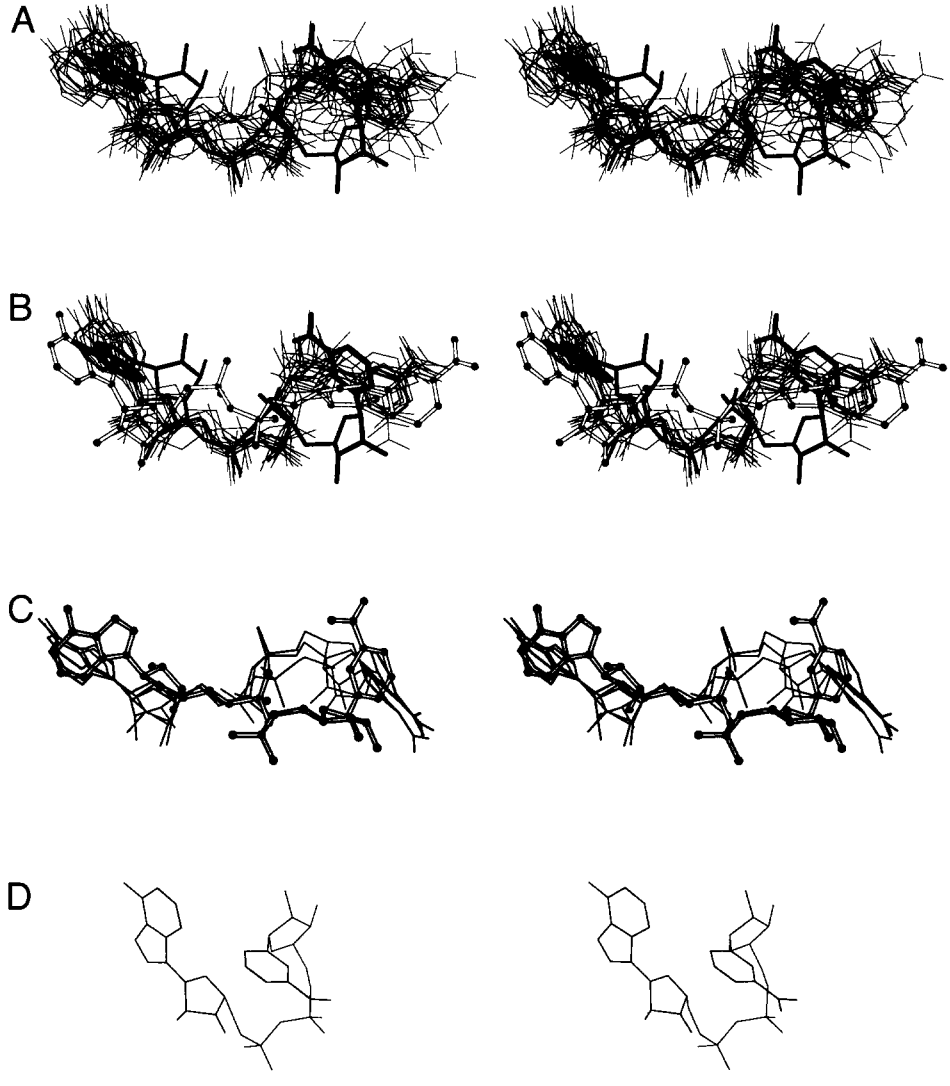

Fig. 4. Superposition of enzyme-bound NAD(P) conformations. All NAD(P) conformations were superimposed to NAD bound to alcohol dehydrogenase (2OHX), as a common reference structure. For NADP structures, the 2′ phosphate is omitted. **A:** Conformations of all enzyme-bound NAD(P)s are shown, except for NADP bound to catalase (8CAT). NAD bound to DT is shown in thick lines. Notice that the conformation of NAD bound to DT is unusual. **B:** Only the conformations of NAD(P) bound to the 14 class 1 Rossmann fold enzymes are shown. The conformation of NADP bound to 6-phosphogluconate dehydrogenase (1PGO) is shown in ball-and-stick representation. Notice that this NADP is more extended than the other class 1 NAD(P) conformations. The conformation of NAD bound to DT is also shown, in thick lines. **C:** Only the conformations of NAD(P) bound to the class 2 enzymes are shown. Notice that although three of the four are highly similar (thin lines), the fourth NAD conformation, NAD bound to dihydrolipoamide dehydrogenase (1LVL), shown in ball-and-stick, is deviant. **D:** The unusual conformation of NADP bound to catalase (8CAT). Notice that the NADP bound to catalase is highly folded, with the adenine and nicotinamide rings separated by only 3.8 Å. The figure was prepared using MOLSCRIPT (Kraulis, 1991).

oxidoreductase enzymes (columns 1–6) and NAD bound to DT (column 7). The RMSD values between the DT-bound NAD conformation and almost all other enzyme-bound NAD(P) conformations are clearly high (the majority are >3.5 Å), compared with the RMSD values between pairs of oxidoreductase-bound NAD(P) conformations (the majority are <3.0 Å).

The most unusual enzyme-bound NAD conformation is NADP bound to the class 5 enzyme catalase (8CAT). The RMSD values between the catalase-bound NADP and the other NAD(P) conformations are all >3.6 Å, and most are >4.0 Å. The conformation of NADP bound to catalase, shown in Figure 4D, is unusual in that it is highly folded. The adenine and nicotinamide rings are separated by only 3.8 Å (C6N to N3A distance), whereas all other enzyme-bound NAD(P) conformations are separated by at least 10 Å. A possible explanation for the unusual conformation of NADP bound to catalase, in terms of the function of catalase, is discussed below.

As shown in Figure 2B, the conformations of NAD(P) bound to the class 1 oxidoreductase enzymes, which have the Rossmann fold, are highly similar. This similarity has been discussed in detail previously (Rossmann et al., 1975; Branden & Eklund, 1980; Grau, 1982; Eklund & Branden, 1987). This trend has been followed by all 14 of the Rossmann fold enzymes deposited in the Brookhaven PDB. The class 1-bound NAD(P) conformations are highly similar

Table 2. *RMSDs in atomic positions (Å) for pairs of NAD(P) molecules bound to proteins*[a]

		Class						
		1	2	3	4	5	6	7
	PDB	2OHX	1GRB	1ADS	1HEX	8CAT	8DFR	1TOX
1	2OHX	—	2.6	2.2	2.3	4.0	2.9	3.8
1	1QOR	**1.8**	3.4	2.8	2.6	3.8	3.1	3.9
1	2HSD	**2.2**	2.9	2.5	3.0	3.8	3.4	3.4
1	1DHR	**0.6**	3.0	2.6	3.2	4.1	3.2	3.2
1	1ENY	**2.2**	2.9	2.6	3.1	3.9	3.2	3.3
1	1GAD	**2.0**	2.4	2.3	2.6	3.8	3.5	3.8
1	1DIH	**0.6**	2.8	2.4	2.4	3.7	3.0	3.8
1	2NAD	**0.6**	2.9	2.4	2.4	3.8	3.0	3.8
1	1PSD	**0.8**	2.9	2.4	2.4	4.0	2.9	3.8
1	2DLD	**1.5**	3.2	2.4	2.4	4.4	2.8	3.6
1	1BMD	**0.8**	3.0	2.6	2.4	3.8	2.9	3.6
1	1HYH	**0.6**	3.0	2.4	2.3	3.9	2.8	3.7
1	9LDT	**0.5**	2.8	2.4	2.4	3.9	2.9	3.6
1	1PGO	**2.1**	2.4	2.2	2.2	5.2	2.4	4.1
2	1GRB	2.7	—	2.0	2.4	4.6	2.6	3.7
2	1TDF	2.6	**1.0**	2.2	2.3	4.5	2.5	3.5
2	2NPX	2.8	**0.6**	2.1	2.6	4.5	2.8	3.7
2	1LVL	3.4	**3.3**	3.3	3.4	4.8	3.0	2.5
3	1ADS	2.2	2.0	—	1.6	4.6	2.9	3.9
4	1HEX	2.3	2.4	1.6	—	4.4	2.1	3.9
4	1IKB	2.9	3.1	3.5	**2.7**	4.6	2.1	2.8
5	8CAT	4.0	4.6	4.6	4.4	—	4.7	4.4
6	8DFR	2.9	2.6	2.9	2.1	4.7	—	3.1
7	1TOX	3.8	3.7	3.9	3.9	4.4	3.1	—

[a]The columns represent a NAD(P) molecule bound to each of the seven distinct classes of NAD(P) binding proteins. RMSD values between two NAD(P) molecules bound to enzymes of the same structural class are in bold.

at the AMP moiety. The NMN portions are also similar and differ primarily in that the nicotinamide ring is found to be either in the syn ($\chi \sim +60$) or in the anti ($\chi \sim -120$) orientation. The RMSD values between pairs of NAD(P) conformations bound to the class 1 enzymes are among the lowest of any in Table 2 (the majority are <2.0 Å), showing the high degree of overall similarity. In Figure 2B, the conformation of NAD bound to DT is also superimposed, in thick lines, to show the difference between the DT-bound NAD conformation and the conformations of NAD(P) bound to the Rossmann fold enzymes.

One Rossmann fold enzyme, 6-phosphogluconate dehydrogenase (1PGO), binds a somewhat different conformation of NADP (Fig. 2B, shown in ball-and-stick representation). This conformation of NADP is clearly more extended than the 13 other conformations of NAD(P) bound to the Rossmann fold enzymes, and could be considered an outlier. Thus, whereas the majority of class 1 Rossmann fold enzymes bind a highly similar conformation of NAD(P), there is one outlier that is more extended.

A high degree of similarity in the conformations of bound NAD(P) molecules is also noticed within the class 2 enzymes (Fig. 4C). Three of the class 2 enzymes, glutathione reductase (1GRB), thioredoxin reductase (1TDF), and NADH peroxidase (2NPX), bind to highly similar NAD(P) conformations, shown in thin lines. NADP bound to thioredoxin reductase (1TDF) and NAD bound to NADH peroxidase (2NPX) superimpose with NADP bound to glutathione reductase (1GRB) to RMSD values of 1.0 and 0.6, respectively. However, one of the class 2 enzyme-bound NAD(P) conformations, NAD bound to dihydrolipoamide dehydrogenase (1LVL), shown in ball-and-stick representation in Figure 4C, is far less similar to the other three. Although the structure of dihydrolipoamide dehydrogenase itself is similar in overall fold to the other three class 2 enzyme structures, it binds to a somewhat different conformation of NAD(P).

The class 3 enzyme aldose reductase (1ADS), which has an $(\alpha\beta)_8$ fold, binds an NADP conformation that is similar to the conformations of NAD(P) bound to the majority of other oxidoreductase enzymes. This can be seen by the low RMSD values in Table 2 (most are <2.5 Å) between NADP bound to aldose reductase (1ADS) and NAD(P) bound to most of the other oxidoreductase enzymes. In contrast, the aldose reductase-bound NADP conformation is less similar to the DT-bound NAD, given that the RMSD between these two is 3.9 Å.

The conformation of NAD bound to the class 4 enzyme 3-isopropylmalate dehydrogenase (1HEX) is also similar to NAD(P) bound to the other oxidoreductase enzymes (majority of RMSDs <3.0 Å), but is not similar to the DT-bound NAD conformation (RMSD = 3.9 Å). The class 6 enzyme dihydrofolate reductase (8DFR) follows a similar trend.

In summary, the superposition of the conformations of NAD(P) bound to the 24 enzymes in Table 1 shows the following. (1) The conformations of NAD(P) bound to DT (1TOX) and catalase (8CAT) are particularly unusual. (2) The conformations of NAD(P) bound to enzymes of related structure (same structural class) are highly similar, with few outliers. This is shown by the

class 1 enzymes with 14 members and 1 outlier, and the class 2 enzymes with 4 members and 1 outlier. (3) In general, the oxidoreductase enzymes, regardless of structural class, bind to similar conformations of NAD(P), as compared to DT, which binds an unusual conformation of NAD. The RMSD values between the DT and oxidoreductase NAD(P) molecules range from 2.5 to 4.1 Å, with a mean of 3.6 Å, whereas between pairs of NAD(P) molecules bound to oxidoreductase enzymes (excluding catalase), the RMSD values range from 0.6–3.5 Å, with a mean of 2.6 Å.

Principal component analysis of enzyme-bound NAD(P) conformations

A more objective way of comparing the conformations of NAD(P) bound to the 24 enzymes in Table 1 is principal component analysis. Principal component analysis is particularly useful for comparing multi-variable systems, and was first employed for comparing multiple protein structures by Diamond (1974). Given the superimposed atomic coordinates (3 × 44 atoms) of each of the NAD(P) molecules in a 3-dimensional space, principal component analysis projects the structures into a generalized, 132-dimensional coordinate space and identifies the linear combination of coordinates that best distinguishes the 3-dimensional structures. The result of such an analysis for the 24 enzyme-bound NAD(P) conformations, projected into two dimensions, is shown in Figure 5. The conformational differences between NAD(P) structures is reflected by their separations in the projection, as near as is possible in two dimensions.

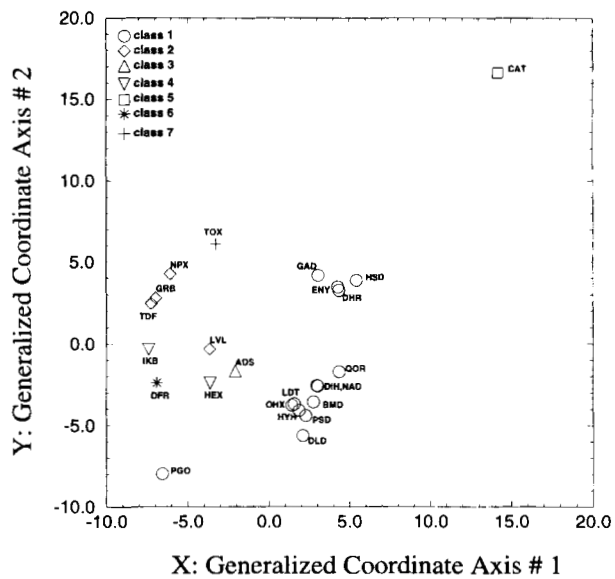

Fig. 5. Principal component analysis: A projection of NAD(P) structures into a generalized coordinate space. Each enzyme class is represented by a different symbol, shown in the upper left corner of the figure. Notice that, in the projection, the 14 class 1 enzyme-bound NAD structures cluster together into two groups, except for PGO, which is deviant. The four class 2 enzyme-bound NAD(P) structures and the two class 5 enzyme-bound NAD(P) structures are also close together in the projection. Also notice that the class 5-bound NADP conformation (NADP bound to catalase) is the furthest removed. The conformation of NAD bound to DT (TOX) is the furthest (except for CAT) in the y direction of the projection.

One obvious feature of the projection is that conformations of NAD(P) bound to enzymes of the same structural class are clustered. This is particularly true for the 14 conformations of NAD(P) bound to the class 1 enzymes. With the exception of NADP bound to 6-phosphogluconate dehydrogenase (PGO), the class 1-bound NAD(P) conformations form two tightly clustered groups. These two groups are distinguished by the χ_N torsion angle: the class 1 NAD(P) conformations in the upper group, at approximately $x = 4$, $y = 4$ (GAD, ENY, DHR, HSD), all have the nicotinamide ring in the syn orientation, whereas the remainder of class 1-bound NAD(P) conformations, in the lower group, all have the nicotinamide ring in the anti orientation. The conformation of NADP bound to 6-phosphogluconate dehydrogenase (PGO), which was shown in Figure 4B to be unusually extended, does not cluster with either of these groups of class 1 NAD(P) conformations.

Like the class 1-bound NAD(P) conformations, the class 2-bound NAD(P) conformations are close together in the projection. The conformation of NAD bound to dihydrolipoamide dehydrogenase (LVL), although close to the other three class 2-bound NAD(P) conformations (GRB, TDF, NPX), is somewhat removed. This is consistent with the superposition of class 2-bound NAD(P) conformations (Fig. 4C), which shows that the LVL NAD is an outlier from the other class 2 members. The conformations of NAD(P) bound to the two class 3 enzymes, 3-iso propyl malate dehydrogenase (HEX) and isocitrate dehydrogenase (1HEX), are also close together in the projection.

The furthest removed NAD(P) conformation in the projection, and thus the most deviant, is NADP bound to catalase (CAT), in the upper right corner. This is consistent with the RMSDs in Table 2, which show that NADP bound to catalase is the most deviant of all of the enzyme-bound NAD(P) conformations. Of note, the conformation of NADP bound to catalase, which is highly folded, and the conformation of NADP bound to 6-phosphogluconate dehydrogenase (PGO), which is the most extended, are in opposite corners of the projection.

Although the conformation of NAD bound to DT (TOX) is not nearly as removed as NADP bound to catalase (CAT), it is somewhat removed. The DT-bound NAD conformation is the furthest (next to CAT) along the y direction of the projection. Thus, although the DT-bound NAD conformation is not nearly as unusual as the catalase-bound NADP conformation, it is distinctive.

In summary, principal component analysis, like least-squares superposition, shows that, in general, enzymes that have similar structures (belonging to the same structural class), bind to similar conformations of NAD(P). The two exceptions, LVL (class 2) and PGO (class 1), are shown to be outliers both by principal component analysis and by superposition. Principal component analysis also shows that NADP bound to catalase, which is highly folded, is the most unusual of known enzyme-bound NAD(P) conformations.

Analysis of enzyme-bound NAD(P) torsion angles

The least-squares superposition and principal component analysis have shown that the conformation of NAD bound to DT is distinctive, when compared to the majority of NAD(P) conformations bound to the oxidoreductase enzymes. In order to describe, in more detail, what specific features of the DT-bound NAD conformation are distinctive, we have analyzed all enzyme-bound NAD(P) torsion angles (Fig. 6) and other conformational parameters (Table 3).

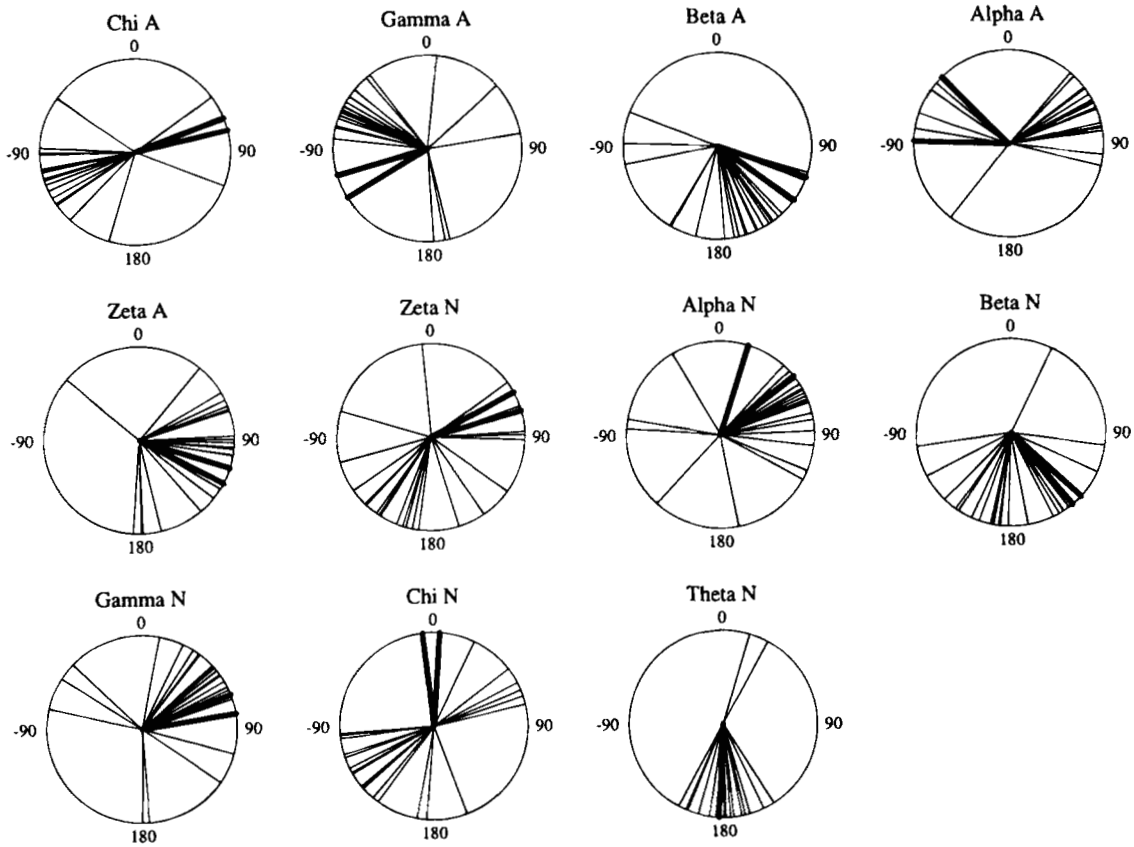

Fig. 6. Torsion angles of the 25 enzyme-bound NAD structures. The 25 values for each torsion angle are plotted on separate pie charts. Values for NAD from the two independently determined DT-NAD complexes are shown in thick lines, and values for the remaining 23 NAD(P) conformations are shown in thick lines. Torsion angles are defined in Figure 3.

Figure 6 shows the torsion angles of all of the enzyme-bound NAD(P) conformations listed in Table 1. The torsion angles are defined in Figure 3. For each torsion angle, the values for all 25 NAD(P) structures are plotted in a pie chart, with the DT-bound NAD torsion angles in thick lines. It is important to note that the enzyme-bound NAD(P) torsion angles are derived from relatively low-resolution crystal structures, as compared to typical "small" molecule crystal structures. The resolution of NAD(P)-bound enzyme crystal structures in Table 1 ranges from 1.6 Å to 2.8 Å. Thus, in many cases, the torsion angles may not be determined accurately. In addition, the geometrical restraints used commonly in the refinement of most protein structures (and bound ligands such as NAD) can have a significant affect on the geometry of the final, refined structure. However, an estimate of the precision with which the torsion angles can be determined from a 2.3-Å crystal structure can be assessed for the DT-NAD complex, because there are two independently determined DT-NAD complexes of the crystal structure (there are two monomers per asymmetric unit of the crystal). The two independently determined values for each torsion angle of the DT-bound NAD conformation differ by an average of 15°.

As seen in Figure 6, most of the torsion angles of the conformation of NAD bound to DT are not particularly unusual. The β_A, α_A, ζ_A, ζ_N, α_N, β_N, γ_N, and θ_N torsion angles all have values that are in regions that are preferred by the other 23 enzyme-bound NAD(P) conformations. Three of the DT-bound NAD torsion angles, however, χ_A, χ_N, and γ_A, have values that are not in preferred regions.

The χ_A torsion angles of 69° and 77° for the two independently determined DT-bound NAD conformations place the adenine ring of NAD bound to DT in the unusual syn orientation. With the exception of NADP bound to quinone oxido-reductase (1QOR) and NADP bound to isocitrate dehydrogenase (1IKB), all of the enzyme-bound NAD(P) conformations have the adenine ring in the anti orientation (χ_A = −90 to 180°). For purines such as adenine, the syn conformation is disfavored due to steric overlap between the six-membered ring of the base and the ribose (Saenger, 1984). However, this strain can be relieved partially if the ribose is in the C2′-endo conformation, as is the case for NAD bound to DT (1TOX) and NADP bound to isocitrate dehydrogenase (1IKB), but not for NADP bound to quinone oxido-reductase (1QOR). From an analysis of crystal structures of both unbound ("free") nucleotides as well as protein-bound nucleotides (Moodie & Thornton, 1983), it has been shown that the anti conformation (χ_A = −60 to −180°) is preferred strongly for unbound adenine nucleotides, and preferred almost exclusively for adenine nucleotides bound to proteins. Thus, in DT, NAD is bound such that favorable interactions between NAD and residues of DT force the adenine ring to be in the unfavorable syn orientation. The syn orientation of the adenine ring is one unusual feature of the conformation of NAD bound to DT.

The γ_A torsion angle of NAD bound to DT, about C3′A-C4′A-C5′A-O5′A (see Fig. 3), is also unusual, when compared to other enzyme-bound NAD(P) γ_A torsion angles. For the two independent determinations of NAD bound to DT, γ_A is at −106 and −121°, whereas for most of the other enzyme-bound NAD(P)

Table 3. *Conformational parameters of enzyme-bound NAD(P) conformations*[a]

Class	PDB	PA-N9A	PA-C4′A	PN-N1N	PN-C4′N	C6A-C2N	α (degrees)
1	2OHX	6.9	3.8	5.6	3.9	15.1	−55
1	1QOR	6.9	3.4	5.5	3.9	13.6	−15
1	2HSD	6.6	3.7	5.4	4.0	14.0	−78
1	1DHR	7.0	4.0	5.1	3.9	14.6	−77
1	1ENY	7.2	4.0	5.3	3.9	15.0	−33
1	1GAD	7.0	3.7	4.9	3.9	15.1	−57
1	1DIH	6.7	3.9	5.5	3.9	14.2	−58
1	2NAD	6.9	3.8	5.7	3.9	14.7	−55
1	1PSD	7.2	4.0	6.0	3.8	14.9	−71
1	2DLD	4.9	3.3	6.5	3.8	14.5	−34
1	1BMD	6.9	3.8	6.0	4.0	14.0	−55
1	1HYH	6.9	3.8	5.6	3.9	14.8	−56
1	9LDT	7.2	4.0	5.7	3.9	14.8	−55
1	1PGO	5.8	3.6	7.2	3.7	17.8	−131
2	1GRB	6.8	3.8	5.7	3.9	17.5	176
2	1TDF	6.9	3.8	5.4	3.8	17.6	−174
2	2NPX	7.0	3.8	5.6	3.9	17.3	176
2	1LVL	7.2	4.0	5.7	3.4	14.5	−159
3	1ADS	6.0	3.9	5.2	3.6	16.6	133
4	1HEX	4.9	4.0	5.9	3.9	15.6	158
4	1IKB	7.4	3.6	5.5	4.1	16.3	5
5	8CAT	7.2	3.9	5.1	3.9	8.3	11
6	8DFR	5.4	3.9	6.2	3.6	15.5	155
7	1TOX1	6.8	3.6	4.7	3.8	12.4	144
7	1TOX2	7.1	3.7	4.7	3.9	12.5	167

[a]These parameters (Webb et al., 1973) refer to distances (colums 3–7) between atoms shown in Figure 3 and the hypothetical torsion angle α, defined in the text, which describes the relationship between the pyrophosphate of NAD(P) and the bases.

conformations, γ_A is usually near −60° or, in some cases, near 60 or 180°. For unbound nucleotides, the torsion angle γ is found near −60, +60, or 180, resulting in a staggered configuration. The γ_A value near −115° for NAD bound to DT results in the unstable eclipsed configuration. Thus, NAD is bound to DT such that favorable interactions between NAD and the protein force the γ_A torsion angle to be at an energetically unfavorable value. The unfavorable γ_A (−115°) and χ_A (74°) torsion angles of NAD bound to DT are distinctive features that, in part, account for the unusual AMP conformation of DT-bound NAD seen in the superposition in Figure 4A.

The χ_N torsion angle about the N-glycosidic bond of the NMN portion of NAD bound to DT is also unusual. For NAD bound to DT, χ_N is close to 0°, with independently determined values of 4.1 and −6.4°. This places the nicotinamide ring in approximately the syn orientation, with the carboxamide group of the nicotinamide ring over the N-ribose. The other 23 enzyme-bound NAD(P) conformations have χ_N values ranging from 26 to 77° (syn) and from −94 to 160° (anti). Thus, the DT-bound NAD $\chi_N \sim 0°$ is outside of the preferred syn range. For unbound nucleotides, the χ torsion angles derived from high-resolution crystal structures (Saenger, 1984) show strong preferences for values near either 60° (syn) or −120° (anti). Thus, the χ_N torsion angle of NAD bound to DT is found to be unusual among both unbound and enzyme-bound nucleotides, and is likely to be energetically unfavorable. Because DT catalyzes the cleavage of NAD at the N-glycosidic bond between N1N and C1′N, the unusual $\chi_N \sim 0°$ torsion angle about this bond may be relevant to DT's unusual function, as is discussed below.

Other conformational parameters of enzyme-bound NAD(P) structures

In addition to the torsion angles in Figure 6, we have also analyzed a set of five distances and a hypothetical torsion angle defined previously (Webb et al., 1973) for each of the 24 enzyme-bound NAD(P) conformations (Table 3). The five distances are PA-N9A, PA-C4′A, PN-N1N, PN-C4′N, and C6A-C2N. The hypothetical torsion angle α is defined by AN9-PA-PN-N1N, and describes the relationship between the pyrophosphate of NAD(P) and the bases; if the bases are on the same side of the pyrophosphate group, then α is ~0°, and if the bases are on opposite sides of the pyrophosphate, α is ~180°.

The PA-N9A and PN-N1N distances reflect the position of the O5′ phosphate relative to the base for each of the individual nucleotides in a particular conformation of NAD(P). As seen in Table 3 for the 24 enzyme-bound NAD(P) structures, the PA-N9A distances range from 4.9 Å (closed AMP conformation) to 7.4 Å (open AMP conformation). For the majority of enzyme-bound NAD(P) conformations, including NAD bound to DT, the PA-N9A distance is toward the high end [19/24 NAD(P)s have PA-N9A > 6.5 Å]. Thus, for most enzyme-bound NAD(P) structures, including NAD bound to DT, the AMP portion is in a more or less extended conformation.

In contrast, the PN-N1N distances in Table 3 for the NMN portion of the enzyme-bound NAD(P) conformations are toward the low end. Although the PN-N1N distances range from 4.7 to 7.2 Å, 22/24 of the NAD(P)s have PN-N1N <6.2 Å. Accordingly,

for the majority of enzyme-bound NAD(P) structures, the NMN portion is in a somewhat more closed conformation. The conformation of NAD bound to DT has the shortest PN-N1N distance (4.7 Å) of all of the enzyme-bound NAD(P) conformations, and thus the NMN portion of NAD bound to DT is in an unusually closed conformation. The unusually folded conformation of the NMN portion of NAD bound to DT may be relevant to DT's unusual function, as is discussed below.

The PA-C4′A and PN-C4′N distances, which range from 3.3 to 4.0 Å, and 3.4 to 4.1 Å, respectively, show little spread and are not particularly informative.

The C6A-C2N distance, which approximates the distance between the adenine and nicotinamide rings, has been used frequently as a measure of the overall extension of a particular NAD(P) conformation (Webb et al., 1973; Rossmann et al., 1975; Eklund et al., 1984). For the 24 enzyme-bound NAD(P) conformations compared here, the C6A-C2N distances range from 8.3 to 17.8 Å. This distance is greatest (17.8 Å) for NADP bound to 6-phosphogluconate dehydrogenase (1PGO), and shortest (8.3 Å) for NADP bound to catalase (8CAT). NAD bound to DT has the second-shortest C6A-C2N distance (12.4 Å). Thus, the conformation of NAD bound to DT is unusually closed (less extended) when compared to the conformations of NAD(P) bound to the oxidoreductase enzymes (except for catalase).

The hypothetical torsion angle α is also informative. This conformational parameter is one of the best at distinguishing the conformations of NAD(P) bound to enzymes of different structural classes. The conformations of NAD(P) bound to the class 1 enzymes have α angles in the range of -15 to $-55°$. One exception is NADP bound to 6-phosphogluconate dehydrogenase (1PGO), which has an α angle of $-131°$. This NADP conformation was also identified above by superposition and by principal component analysis as being different from the other class 1-bound NAD(P) conformations. The conformations of NAD(P) bound to the four class 2 enzymes have α angles in the range of -174 to $176°$, except for NAD bound to dihydrolipoamide dehydrogenase (1LVL), which has an α angle of $-159°$. This NADP conformation was identified above, by RMSD and principal component analysis, as being an outlier from the other three class 2 NAD(P) conformations. For NAD bound to DT, $\alpha = 144°$, indicating that the bases are roughly on opposite sides of the pyrophosphate group.

In summary, the conformational parameters defined previously (Webb et al., 1973), shown in Table 3, are useful for comparing the 24 enzyme-bound NAD(P) conformations. The conformation of NAD bound to DT has unusually short PN-N1N and C6A-C2N distances, indicating that the DT NAD conformation is unusually folded (as opposed to extended), particularly for the NMN portion.

Discussion

In this study, we ask the question: is the conformation of NAD, when bound to DT, relevant to DT's function as an ADP-ribosyltransferease? It has been well established that the glutamic acid residue 148 of DT plays an essential role in catalysis of the ADP-ribosylation of EF-2 (Wilson et al., 1990), most probably through electrostatic interactions. It is possible, however, that the conformation of NAD when bound to DT could also be a contributing factor.

There are at least two conceivable ways in which the conformation of NAD, when bound to DT, could be relevant to catalysis of the ADP-ribosylation reaction. First, in binding to NAD, DT could place strain on the N-glycosidic bond, between the nicotinamide ring and the N-ribose. For example, the N-glycosidic bond of NAD, when bound to DT, could be elongated and hence destabilized, favoring cleavage. Second, in binding to NAD, DT could expose and orient the anomeric C1′N atom of NAD for reaction with the diphthamide residue of EF-2.

Unfortunately, because the crystal structure of DT was determined at a resolution of only 2.3 Å (typical of crystal structures of proteins), the precise geometry (bond angles and bond lengths) of the final, refined NAD conformation most probably reflects the geometrical restraints put into the crystallographic refinement, to a greater extent than the actual structure. Thus, from the 2.3-Å resolution crystal structure of the DT-NAD complex, it cannot been determined whether the N-glycosidic bond of NAD is elongated when bound to DT, because the degree of elongation (0.1–0.3 Å) would not be significant compared to the mean coordinate error of the crystal structure (~0.4 Å). A determination of the precise geometry of the N-glycosidic bond of NAD, when bound to DT, would require a crystal structure determined at exceptionally high resolution (>1.5 Å), and also with an exceptional *R*-factor (~15% or below).

In the absence of a highly accurate crystal structure of the DT-NAD complex, one approach to investigate whether or not the conformation of NAD when bound to DT is relevant to DT's function as an ADP-ribosylating enzyme is by comparison with other enzyme-bound NAD conformations. In this study, the conformation of NAD bound to DT has been compared to the conformations of NAD(P) bound to 23 enzymes that catalyze oxidoreductase reactions. Because DT catalyzes an ADP-ribosylation reaction involving cleavage of the N-glycosidic bond of NAD, whereas the 23 oxidoreductase enzymes use NAD(P) as a cofactor for hydride transfer from the C4 position of the nicotinamide ring, one might expect to find distinctive features of the conformation of NAD bound to DT that could be relevant to DT's distinct function as an ADP-ribosylating enzyme.

Two unusual features of the conformation of NAD bound to DT stand out as being possibly relevant to catalysis: (1) the $\chi_N \sim 0°$ torsion angle about the scissile, N-glycosidic bond, and (2) the highly folded conformation of the NMN portion, with an unusually short PN-N1N distance (Table 3). For the two independently determined conformations of NAD bound to DT, the torsion angle χ_N is 4.1 and $-6.4°$. Although the resolution of the DT-NAD crystal structure is only 2.3 Å, because these two values were determined independently, the actual χ_N torsion angle for NAD bound to DT is likely to be close to 0°. The unusual $\chi_N \sim 0°$ torsion angle falls outside of the preferred syn and anti ranges, and is not seen in any of the other enzyme-bound NAD conformations. The short distance between the PN and N1N atoms of the NMN portion of NAD bound to DT is also unusual. For NAD bound to DT, this distance is 4.7 Å, whereas for the 23 oxidoreductase enzymes, the PN-N1N distance ranges from 4.9 to 7.2 Å, with a mean value of 5.7 Å. Thus, the NMN portion of NAD bound to DT is in an unusually folded, or "closed" conformation.

One possible explanation for the unusual $\chi_N \sim 0°$ torsion angle and the highly folded conformation of the NMN portion of NAD bound to DT could be that such a conformation exposes and orients the C1′N atom of NAD for nucleophilic attack by the incoming diphthamide residue of the EF-2 substrate. Folding the nicotinamide ring of NAD back toward the N-phosphate, and orienting the nicotinamide ring approximately coplanar with the N-ribose ($\chi_N \sim 0°$) could serve to expose the C1′N atom of NAD maxi-

mally. This would allow sufficient space for reaction of the C1'N atom of NAD with the imidazole ring of the diphthamide residue of EF-2, and also for interaction with the carboxylate group of the catalytic Glu 148 of DT. Indeed, in the crystal structure of DT bound to NAD, the carboxylate group of Glu 148 is positioned 4.0 Å from the C1'N atom of NAD.

A second possible explanation for the unusual $\chi_N \sim 0°$ torsion angle and short PN-N1N distance in NAD bound to DT is that NAD could be bound to DT in a strained conformation, favoring cleavage of the N-glycosidic bond. The $\chi_N \sim 0°$ torsion angle could be unfavorable energetically, due to steric overlap between the lone pair electrons of the O4'N atom of the N-ribose, and the hydrogen attached to the C2N atom of the nicotinamide ring. Such steric overlap could lead to elongation of the N-glycosidic bond. In analyses of high-resolution crystal structures of pyrimidine and purine nucleosides and nucleotides, the N-glycosidic bond length was found to be correlated with the χ_N torsion angle (Lin et al., 1971; Lo et al., 1975; Saenger, 1984). The N-C bond distance was found to be a minimum (1.43 Å) at values of χ_N near the preferred anti and syn ranges, and a maximum (1.52 Å) at χ_N near 0° or 180°. The lengthening of the N-glycosidic bond at χ_N values near 180° was attributed to steric interactions between the O4' atom and the hydrogen atom attached to C6 of uridine, for example (Saenger, 1984). Because similar interactions would be present in NAD, between the hydrogen atoms at the C2- and C6- positions of the nicotinamide ring, and O4' of the ribose, the $\chi_N \sim 0°$ torsion angle could cause a similar elongation of the N-glycosidic bond in NAD. In this way, when NAD is bound to DT, the $\chi_N \sim 0°$ torsion angle could be a factor, in addition to electrostatic interactions of the catalytic Glu 148 of DT, which contributes to cleavage of the N-glycosidic bond.

In addition, the observation that in NAD bound to DT the PN-N1N distance is the shortest of known enzyme-bound NAD conformations could be an indication that the NMN portion of NAD bound to DT is in a strained conformation. Thus, by imposing a strained conformation of the NMN portion of NAD, DT could promote cleavage of the N-glycosidic bond.

In summary, our comparative study has shown that the $\chi_N \sim 0°$ torsion angle and 4.7 Å PN-N1N distance are features of the conformation of NAD bound to DT that are not observed for the conformations of NAD(P) bound to 23 oxidoreductase enzymes, which do not catalyze cleavage of the N-glycosidic bond. Because these features are unique to NAD bound to DT, and because they affect the geometry of NAD about the scissile bond, they could possibly be relevant to DT's unique function as an ADP-ribosylating enzyme. However, to show definitively to what extent these unusual features of the conformation of NAD bound to DT contribute to catalysis of the ADP-ribosylation reaction, high-resolution (~1.5 Å) crystal structures of DT bound to NAD and of the ternary complex between DT, NAD, and EF-2, are needed.

In addition to demonstrating unusual features of NAD bound to DT that may be relevant to DT's function, the comparison of NAD conformations in this study shows several other important differences and similarities, not related to DT's distinct function. As shown in the superposition in Figure 4A and in the RMSDs in Table 2, the overall conformation of NAD bound to DT is unusual when compared to the conformations of NAD(P) bound to the 23 oxidoreductase enzymes. The DT-NAD conformation is most unusual in that it is the least extended (except for NADP bound to catalase) of all of the enzyme-bound NAD(P) conformations (Fig. 4A). This is seen by the unusually short C6A-C2N distance of 12.5 Å for NAD bound to DT (Table 3). In addition, the unusual $\chi_A \sim 74°$ and $\gamma_A \sim 109°$ torsion angles give rise to a conformation for the AMP portion of NAD bound to DT, which differs significantly from the other 23 enzyme-bound NAD(P) structures, as seen in the superposition in Figure 4A.

The unusual overall conformation of NAD bound to DT most likely reflects the structure of DT, which is unusual among the NAD-binding proteins. In DT, the NAD binding site is formed at the interface of two antiparallel β-sheets (Fig. 2). NAD binds to the surface of each of the β-sheets where they meet one another at approximately a right angle. In contrast to DT, although the 23 oxidoreductase enzymes in Table 1 have been classified (according to the SCOP database) into five different structural groups on the basis of their folding topologies, they all are of the α/β type, and they all have a similar NAD(P) binding site. In each case, the NAD(P) binding site is formed at the C-terminal end of a parallel β-sheet, with the exception of the class 4 enzymes isocitrate dehydrogenase (1IKB) and 3-isopropylmalate dehydrogenase (1HEX), in which the β-sheet is mixed parallel and antiparallel (Fig. 1), and the class 5 enzyme catalase, which is discussed below. Thus, the similar NAD(P) binding sites of the majority of oxidoreductase enzymes most probably account for the similar conformations of NAD(P) to which they bind.

Other ADP-ribosylating enzymes, whose structures have been determined by X-ray crystallography, have an NAD binding site that is structurally homologous to that of DT. In the crystal structure of the catalytic domain of *Psuedomonas* exotoxin A (ETA) bound to the NAD analogue β-methylene-thiazole-4-carboxamide adenine dinucleotide (β-TAD), the NAD analogue adopts a conformation that is highly similar to that of NAD bound to DT (Li et al., 1996). This can be seen in a superposition of the DT-NAD complex with the ETA-β-TAD complex, shown in Figure 7. This superposition is based only on the Cα atoms of the two catalytic protein domains, which align to an RMSD of 2.1 Å for 121 pairs. However, because β-TAD, the NAD analogue complexed to exotoxin A, is significantly different chemically from NAD, it was not possible to include the conformation of β-TAD bound to ETA in the comparative methods used in this study. This result strongly suggests that all ADP-ribosylating enzymes, at least the ADP-ribosylating toxins whose structures are homologous, will bind a conformation of NAD that is highly similar to NAD bound to DT and ETA.

Another important result of the comparison of enzyme-bound NAD(P) conformations in this study is that enzymes of the same structural class bind to particularly similar conformations of NAD(P). Although this result is not unexpected and has been shown previously for several Rossmann fold (class 1) oxidoreductase enzymes (Rossmann et al., 1975; Branden & Eklund, 1980; Grau, 1982; Eklund & Branden, 1987), the comparisons in this study are based on a greater number of structures (all deposited in the PDB), and demonstrate more completely to what extent enzymes of related structure bind to similar conformations of NAD. In comparing the 24 enzyme-bound NAD conformations by structural superposition, RMSDs of atomic positions, principal component analysis, and the hypothetical torsion angle α (Table 3), this trend is demonstrated for 14 class 1 Rossmann fold enzymes, 4 class 2 enzymes, and 2 class 4 enzymes. Importantly, the comparisons in this study also reveal two enzymes that are outliers, because they bind NAD(P) conformations that are significantly distinct from the NAD(P) conformations bound to other eznymes of their respective structural classes. These are 6-phosphogluconate dehydrogenase (1PGO) of

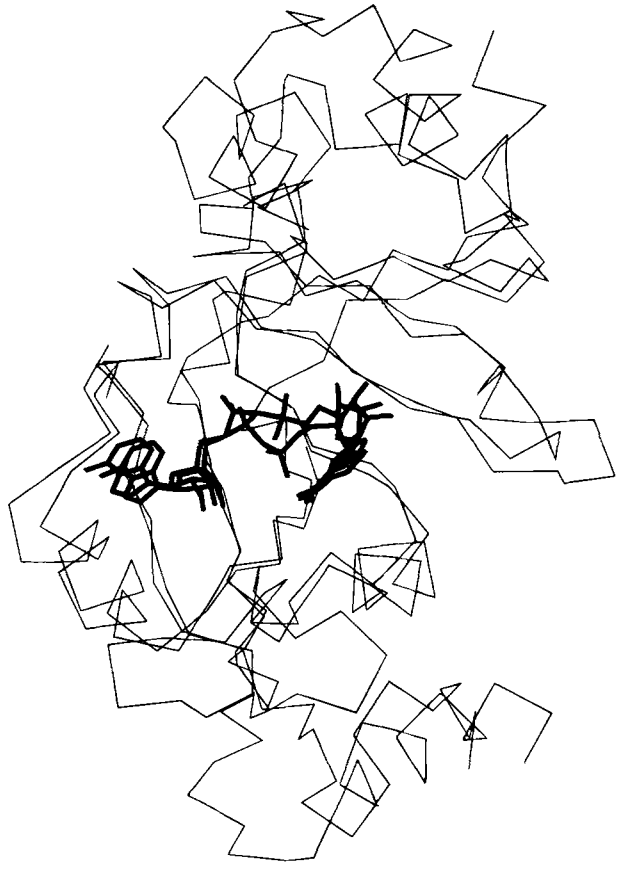

Fig. 7. Superposition of the catalytic domain of *Pseudomonas* exotoxin A (ETA) bound to an NAD analogue [PDB entry 1AER (Li et al., 1996)] and the catalytic domain of diphtheria toxin (DT) bound to NAD [PDB entry 1TOX (Bell & Eisenberg, 1996)]. The Cα-traces of the catalytic domains of ETA and DT are shown in thin lines. NAD bound to DT, and the NAD analogue bound to ETA are shown in thick lines. The NAD analogue, β-methylene-thiazole-4-carboxamide adenine dinucleotide (β-TAD), differs from NAD in that a five-membered thiazole ring replaces the nicotinamide ring, a C-glycosidic bond replaces and N-glycosidic bond, and a carbon replaces the β-oxygen in the pyrophosphate. The superposition is based only on the Cα atoms of the two proteins. For residues 18–187 of DT, and residues 437–585 of ETA, 121 pairs of Cα atoms align to an RMSD of 2.1 Å. Notice that the conformations of NAD bound to DT, and the NAD analogue bound to ETA are similar. Also notice that the structures of ETA and DT are highly similar in the NAD binding regions.

class 1 and dihydrolipoamide dehydrogenase (1LVL) of class 2. However, from this comparative study, it cannot be explained why these two are outliers.

The principal component analysis is particularly useful for demonstrating the high degree of similarity among conformations of NAD(P) bound to enzymes of the same structural class, because NAD conformations bound to enzymes of the same structural class are, in general, closely positioned in the two-dimensional projection of enzyme-bound NAD(P) structures. Moreover, principal component analysis shows the two outliers, PGO of class 1 and LVL of class 2, as in the projection, these NAD(P) conformations are removed significantly from the other NAD(P) conformations bound to enzymes of the same structural class. To our knowledge, principal component analysis has not been utilized previously for comparing the conformations of NAD(P) bound to enzymes, or other enzyme-bound substrates or cofactors, and may be useful in comparing enzyme-bound conformations of molecules such as ADP, ATP, etc., where a significant number of crystal structures are available. As a greater number of structures of enzyme–substrate complexes are deposited in the PDB in the future, principal component analysis may become increasingly useful for comparative studies.

Finally, the enzyme catalase (8CAT), which binds a very unusual, highly folded conformation of NADP, also has a structure that is unusual among the oxidoreductase enzymes. In catalase, NADP is bound between an entirely α-helical domain and an eight-stranded, antiparallel β-barrel. The conformation of NADP bound to catalase is most unusual in that the adenine and nicotinamide rings are separated by only 3.8 Å at the closest point, between C6N and N3A. One possible explanation for this unusual feature is the function of the NADP cofactor for catalase. In catalase, an electron is transferred from a bound NADPH molecule, 20 Å through the interior of the protein to a heme group. It has been suggested that the adenine ring of NAD lies along a possible pathway of electron transfer between the nicotinamide C4 atom of NAD and the heme iron center (Gouet et al., 1995). This could possibly explain why catalase binds a highly unusual conformation of NADP, in which the adenine and nicotinamide rings are separated by only 3.8 Å.

Materials and methods

All of the distinct NAD(P)-binding proteins whose structures have been determined in complex with β-NAD or β-NADP and deposited in the Brookhaven Protein Data Bank have been included in this comparative study. These enzymes are listed in Table 1. In cases where structures are available from more than one species for a particular enzyme–NAD complex, only the highest-resolution structure has been included in this study. For enzymes with multiple subunits, only one NAD(P) conformation has been included. The structural classification of enzymes in Table 1 is based on folding topologies, and was taken directly from the SCOP database (Murzin et al., 1995). The class numbers have been assigned by the present authors.

References for each of the 24 crystal structures listed in Table 1 are as follows: 1QOR (Thorn et al., 1995); 2HSD (Ghosh et al., 1994); 1DHR (Varughese et al., 1992); 1ENY (Dessen et al., 1995; 1GAD (Duee et al., 1996); 1DIH (Scapin et al., 1995); 2NAD (Lamzin et al., 1994); 1PSD (Schuller et al., 1995); 1BMD (Kelly et al., 1993); 1HYH (Niefind et al., 1995); 1PGO (Adams et al., 1994); 1GRB (Karplus & Schulz, 1989); 1TDF (Waksman et al., 1994); 2NPX (Stehle et al., 1993); 1LVL (Mattevi et al., 1992); 1ADS (Wilson et al., 1992); 1HEX (Hurley & Dean, 1994); 1IKB (Stoddard et al., 1993); 8CAT (Fita & Rossmann, 1985); 1TOX (Bell & Eisenberg, 1996). References for 2OHX, 2DLD, 9LDT, and 8DFR could not be found.

For each superposition shown in Figure 4, all NAD(P) structures were aligned to that of NAD bound to alcohol dehydrogenase (2OHX) using a least-squares algorithm (Kabsch, 1976) implemented by X-PLOR (Brünger, 1990). For the suppositions and other calculations, the 3′-phosphate of NADP was omitted. RMSD values in Table 2 and torsion angles in Figure 6 were also calculated using X-PLOR. Principal component analysis (Diamond, 1974) was performed on the Cartesian coordinates of the 24 NAD(P) conformations using locally written software. The five distances and the hypothetical torsion angle α in Table 3 were measured using FRODO (Jones, 1978).

Acknowledgments

We thank NIH grant GM-31299 for support, and Dr. R. John Collier for useful discussions.

References

Adams MJ, Ellis GH, Gover S, Naylor CE, Phillips C. 1994. Crystallographic study of coenzyme, coenzyme analogue, and substrate binding in 6-phosphogluconate dehydrogenase: Implications for NADP specificity and the enzyme mechanism. *Structure (Lond) 2*:651–668.

Bell CE, Eisenberg D. 1996. Crystal structure of diphtheria toxin bound to nicotinamide adenine dinucleotide. *Biochemistry 35*:1137–1149.

Branden CI, Eklund H. 1980. Structure and mechanism of liver alcohol dehydrogenase, lactate dehydrogenase and glyceraldehyde-3-phosphate dehydrogenase. In: Jeffery J, ed. *Dehydrogenases requiring nicotinamide coenzymes*. Basel: Birkhauser Verlag. pp 40–84.

Brünger AT. 1990. *X-PLOR manual version 3.1*. New Haven, Connecticut: Yale University.

Collier RJ. 1975. Diphtheria toxin: Mode of action and structure. *Bacteriol Rev 39*:54–85.

Dessen A, Quemard A, Blanchard JS, Jacobs WR Jr, Sacchettini JC. 1995. Crystal structure and function of the isoniazid target of Mycobacterium tuberculosis. *Science 267*:1638–41.

Diamond R. 1974. Real-space refinement of the structure of hen egg-white lysozyme. *J Mol Biol 82*:371–391.

Duee E, Olivier-Deyris L, Fanchon E, Corbier C, Branlant G, Dideberg O. 1996. Comparison of the structures of wild-type and a N313T mutant of *Escherichia coli* glyceraldehyde 3-phosphate dehydrogenases: Implication for NAD binding and cooperativity. *J Mol Biol 257*:814–38.

Eklund H, Branden CI. 1987. Crystal structure, coenzyme conformations, and protein interactions. In: Dolphin DNY, ed. *Pyridine nucleotide coenzymes*. New York: Wiley. pp 51–98.

Eklund H, Samama JP, Jones TA. 1984. Crystallographic investigations of nicotinamide adenine dinucleotide binding to horse liver alcohol dehydrogenase. *Biochemistry 23*:5982–5996.

Fita I, Rossmann MG. 1985. The NADPH binding site on beef liver catalase. *Proc Natl Acad Sci USA 82*:1604.

Ghosh D, Wawrzak Z, Weeks CM, Duax WL, Erman M. 1994. The refined three-dimensional structure of 3-α,20-β-hydroxysteroid dehydrogenase and possible roles of the residues conserved in short-chain dehydrogenases. *Structure 2*:629–40.

Gouet P, Jouve HM, Dideberg O. 1995. Crystal structure of *Proteus mirabilis* PR catalase with and without bound NADPH. *J Mol Biol 249*:933–954.

Grau UM. 1982. Structural interactions with enzymes. In: Everse J, Anderson B, You KS, eds. *The pyridine nucleotide coenzymes*. New York: Academic Press. pp 135–187.

Hurley JH, Dean AM. 1994. Structure of 3-isopropylmalate dehydrogenase in complex with NAD+: Ligand-induced loop closing and mechanism for cofactor specificity. *Structure 2*:1007–1016.

Jones TA. 1978. A graphics model building and refinement system for macromolecules. *J Appl Crystallogr 11*:268–272.

Kabsch W. 1976. A solution for the best rotation to relate two sets of vectors. *Acta Crystallogr A 32*:922–923.

Kelly CA, Nishiyama M, Ohnishi Y, Beppu T, Birktoft JJ. 1993. Determinants of protein thermostability observed in the 1.9 Å crystal structure of malate dehydrogenase from the thermophilic bacterium *Thermus flavus*. *Biochemistry 32*:3913–3922.

Karplus PA, Schulz GE. 1989. Substrate binding and catalysis by glutathione reductase as derived from refined enzyme:substrate crystal structures at 2.0 Å resolution. *J Mol Biol 210*:163–180.

Kraulis PJ. 1991. MOLSCRIPT: A program to produce both detailed and schematic plots of protein structures. *J Appl Crystallogr 24*:946–950.

Lamzin VS, Dauter Z, Popov VO, Harutyunyan EH, Wilson KS. 1994. Crystal structure of NAD-dependent formate dehydrogenase. *J Mol Biol 236*:759–785.

Li M, Dyda F, Benhar I, Pastan I, Davies DR. 1996. Crystal structure of the catalytic domain of *Pseudomonas* exotoxin A complexed with a nicotinamide adenine dinucleotide analog: Implications for the activation process and for ADP ribosylation. *Proc Natl Acad Sci USA 93*:6902–6906.

Lin GHY, Sundaralingam M, Arora SK. 1971. Stereochemistry of nucleic acids and their constituents. XV. Crystal and molecular structure of 2-thiocytidine dihydrate, a minor constituent of transfer ribonucleic acids. *J Am Chem Soc 93*:1235–1241.

Lo A, Shefter E, Cochran TG. 1975. Analysis of N-glycosyl bond length in crystal structures of nucleosides and nucleotides. *J Pharm Sci 64*:1707–1710.

Lory S, Carroll SF, Bernard PD, Collier RJ. 1980. Ligand interactions of diphtheria toxin I. Binding and hydrolysis of NAD. *J Biol Chem 255*:12011–12015.

Mattevi A, Obmoloua G, Sokatch JR, Betzel C, Hol WGJ. 1992. The refined crystal structure of *Pseudomonas putida* lipoamide dehydrogenase complexed with NAD+ at 2.45 Å resolution. *Proteins Struct Funct Genet 13*:36–351.

Moodie SL, Thornton JM. 1993. A study into the effects of protein binding on nucleotide conformation. *Nucleic Acids Res 21*:1369–1380.

Murzin AG, Brenner SE, Hubbard T, Chothia C. 1995. SCOP: A structural classification of proteins database for the investigation of sequences and structure. *J Mol Biol 247*:536–540.

Niefind K, Hecht HJ, Schomberg D. 1995. Crystal structure of L-2-hydroxyisocaproate dehydrogenase from *Lactobacillus confusus* at 2.2 Å resolution. An example of strong asymmetry between subunits. *J Mol Biol 251*:256–281.

Rossmann MG, Liljas A, Branden CI, Banaszak LT. 1975. Evolutionary and structural relationships among dehydrogenases. *The Enzymes 11*:61–102.

Saenger W. 1984. *Principles of nucleic acid structure*. New York: Springer-Verlag.

Scapin G, Blanchard JS, Sacchettini JC. 1995. Three-dimensional structure of *Escherichia coli* dihydrodipicolinate reductase. *Biochemistry 34*:3502–3512.

Schuller DJ, Grant GA, Banaszak LJ. 1995. The allosteric ligand site in the Vmax-type cooperative enzyme phosphoglycerate dehydrogenase. *Nature Struct Biol 2*:69–76.

Stehle T, Claiborne A, Schulz GE. 1993. NADH binding site and catalysis of NAD peroxidase. *Eur J Biochem 211*:221.

Stoddard BL, Dean A, Koshland DE Jr. 1993. Structure of isocitrate dehydrogenase with isocitrate, nicotinamide adenine dinucleotide phosphate, and calcium at 2.5 Å resolution: a pseudo-Michaelis ternary complex. *Biochemistry 32*:9310–9316.

Thorn JM, Barton JD, Dixon NE, Ollie DL, Edwards KJ. 1995. Crystal structure of *Escherichia coli* quinone oxidoreductase complexed with NADPH. *J Mol Biol 249*:785–799.

Van Ness BG, Howard JB, Bodley JW. 1980. ADP-ribosylation of elongation factor 2 by diphtheria toxin. NMR spectra and proposed structures of ribosyldiphthamide and its hydrolysis products. *J Biol Chem 255*:10710–10716.

Varughese KI, Skinner MM, Witeley JM, Mathews DA, Xuong NH. 1992. Crystal structure of rat liver dihydropteridine reductase. *Proc Natl Acad Sci USA 89*:6080–6084.

Waksman G, Krishna TS, Williams CH Jr, Kuriyan J. 1994. Crystal structure of *Escherichia coli* thioredoxin reductase refined at 2 Å resolution. Implications for a large conformational change during catalysis. *J Mol Biol 236*:800–816.

Webb LE, Hill EJ, Banaszak LJ. 1973. Conformation of nicotinamide adenine dinucleotide bound to cytoplasmic malate dehydrogenase. *Biochemistry 12*:5101–5109.

Wilson BA, Reich KA, Weinstein BR, Collier RJ. 1990. Active-site mutations of diphtheria toxin: Effects of replacing glutamic acid-148 with aspartic acid, glutamine, or serine. *Biochemistry 29*:8643–8651.

Wilson DK, Bohren KM, Gabbay KH, Quiocho FA. 1992. An unlikely sugar substrate site in the 1.65 Å structure of the human aldose reductase holoenzyme implicated in diabetic complications. *Science 257*:81–84.